A strontium isoscape of southwestern Australia and progress toward a national strontium isoscape

Patrice de Caritat[1,2], Anthony Dosseto[3], Florian Dux[3]

[1]Geoscience Australia, GPO Box 378, Canberra ACT 2601, Australia
5   [2]John de Laeter Centre, Curtin University, Bentley WA 6845, Australia
[3]Wollongong Isotope Geochronology Laboratory, School of Earth, Atmospheric and Life Sciences, University of Wollongong, Wollongong NSW 2522, Australia

Correspondence to: Patrice de Caritat (Patrice.deCaritat@curtin.edu.au)

Abstract

10   Strontium isotopes ($^{87}Sr/^{86}Sr$) are widely used tracers in the geosciences. Here we exploit an opportunity to determine $^{87}Sr/^{86}Sr$ ratios on archived fluvial sediment samples from the low-density National Geochemical Survey of Australia. The present study targeted the Yilgarn Craton in southwestern Australia. One hundred and seven new samples were taken from a depth of ~60-80 cm in floodplain deposits at or near the outlet of large catchments (drainage basins). A coarse (< 2 mm) grain-size fraction was air-dried, sieved, milled then digested (hydrofluoric acid + nitric acid followed by aqua regia) to release *total* Sr. The Sr was then separated by chromatography and its $^{87}Sr/^{86}Sr$ ratio determined by multicollector-inductively coupled plasma mass-spectrometry. Results demonstrate a wide range of quite elevated Sr isotopic values (0.7152 to 1.0909, median 0.7560) over the survey area, reflecting a large diversity of source rock lithologies, geological processes and bedrock ages. Spatial distribution of $^{87}Sr/^{86}Sr$ shows coherent (multi-point anomalies and smooth gradients), large-scale (> 100 km) patterns that appear to be broadly consistent with surface geology, regolith/soil type, and/or nearby outcropping bedrock. The most radiogenic sediment values in the Yilgarn region ($^{87}Sr/^{86}Sr$ > 0.8) all come from sites underlain by Archaean bedrock (2500 – 4000 Ma) and almost exclusively felsic intrusive lithologies. Conversely, almost all sites underlain by younger *and* non-granitic bedrock have outlet sediments of a less radiogenic character ($^{87}Sr/^{86}Sr$ < 0.8). Sampling sites underlain by mafic and ultramafic bedrock yield unradiogenic Sr sediment signatures despite their Archaean age. Several sediment $^{87}Sr/^{86}Sr$ results were validated by comparison to previously published whole-rock data from their catchment, for both unradiogenic and radiogenic cases. The new Sr isotopic data are also interrogated in terms of the mineral occurrences (i.e., mineral deposits and/or operating mines) found in their catchment. Several catchments containing mineral resources across a range of commodities stand out as high $^{87}Sr/^{86}Sr$ outliers ($^{87}Sr/^{86}Sr$ > 0.8), whilst over half of the registered mineral resources come from an intermediate, yet still elevated, catchment sediment $^{87}Sr/^{86}Sr$ range ($^{87}Sr/^{86}Sr$ = 0.728 – 0.767). Avenues for future work are proposed, including a national-scale Sr isoscape for Australia. Such an isoscape could be useful in future geological, forensic, archaeological, paleontological and ecological studies. The new spatial Sr isotope dataset for the southwestern Australia region is publicly available (de Caritat et al., 2024; https://dx.doi.org/10.26186/149755).

1 Introduction

Strontium isotope ratios ($^{87}Sr/^{86}Sr$) can be measured in many geological materials as the trace element strontium (Sr) is relatively abundant and readily substitutes for calcium (Ca) in minerals and organic tissues. The $^{87}Sr/^{86}Sr$ of a mineral or rock
35 is a function of (1) its initial and unchanging ^{86}Sr content, (2) its initial rubidium (Rb) content (thus Rb/Sr ratio), and (3) time (e.g. McNutt, 2000). Rubidium substitutes readily for potassium (K) in minerals and is thus relatively common too. As one of the two naturally occurring Rb isotopes, ^{87}Rb, which accounts to 27.8 % of Rb, decays over time (by emitting a negative beta particle) to stable ^{87}Sr ($t_{1/2} = 49.6 \times 10^9$ years), the $^{87}Sr/^{86}Sr$ ratio of that material slowly increases with time (e.g. Rotenberg et al., 2012; Nebel and Stammeier, 2018). During geological processes such as mineral dissolution or precipitation, or biological
40 processes such as bone and tooth growth, the $^{87}Sr/^{86}Sr$ remains constant as there is no isotopic fractionation (e.g. Gosz et al., 1983; Nebel and Stammeier, 2018). These characteristics make the Sr isotopic system very useful in the geosciences, where it has been used for decades in various studies recently reviewed by de Caritat et al. (2023).

Outside of the geosciences, food tracing and provenancing have also been underpinned by the use of Sr isotopes, though in this case relying generally on the *bioavailable* Sr rather than total Sr (e.g. Voerkelius et al., 2010; Di Paola-Naranjo et al.,
45 2011; Vinciguerra et al., 2015; Hoogewerff et al., 2019; Moffat et al., 2020). Anthropological studies have relied on $^{87}Sr/^{86}Sr$ isotope ratios to locate archaeological artefacts or reconstruct ancient human behaviours (e.g. Frei and Frei, 2013; Willmes et al., 2014, 2018; Adams et al., 2019; Pacheco-Forés et al., 2020; Joannes-Boyau et al., 2021; Washburn et al., 2021). Animal migration studies have also relied on Sr isotope data (e.g. Koutamanis et al., 2023; Price et al., 2017). More recently, large-scale compilations and machine-learned predictions of the $^{87}Sr/^{86}Sr$ variations up to the continental and even global scale have
50 been proposed (e.g. Bataille et al., 2014, 2018, 2020).

Strontium isotope landscape maps ('isoscapes') provide the fundamental context required for the interpretation of more detailed scientific research about processes or provenance. Despite the plethora of research using Sr isotopes to address various scientific questions, very few Sr isoscapes exist in the southern hemisphere, particularly for soils or covering large swathes of the Earth's surface (see Bataille et al., 2020). Three exceptions to this in Australia are (1) the work by Adams et al. (2019),
55 which reported $^{87}Sr/^{86}Sr$ in plant, soil, and biota over ~300 000 km^2 on the Cape York Peninsula in Australia; and the recently published Sr isoscapes of (2) inland southeastern Australia (~500 000 km^2) (de Caritat et al., 2022) and (3) northern Australia (~1 500 000 km^2) (de Caritat et al., 2023). The present study affords an opportunity to further redress this deficiency and reduce the northern-hemisphere bias in future global $^{87}Sr/^{86}Sr$ models. It also pertains to a land surface that has not been rejuvenated by recent glaciation, consisting of over 85 % regolith or weathered material (Wilford, 2012), and as a result is
60 abundant in minerals such as kaolinite, illite-smectite, goethite and hematite. The choice of total rather than bioavailable Sr as the focus of this work was driven by an emphasis on geological sources and processes.

2 Setting

The study area in southwestern Australia focusses on the Yilgarn Craton in Western Australia, roughly between 25 and 35 °S and between 115 and 125 °E (Figure 1), bordered to the west by the Indian Ocean and to the south by the Southern Ocean. The climate zone is described as 'Hot dry summer, cold winter' (BOM, 2024a) and the major Koeppen climate zones range from 'Temperate' in the southwest corner of the study area to 'Grassland' and 'Desert' toward the northeast as aridity increases (BOM, 2024b). The 10-year (1996-2005) average minimum and maximum temperatures range from 9 to 15 °C and from 21 to 30 °C, respectively (BOM, 2024c). Average annual rainfall over the four-year period to November 2009 (when the bulk of the sampling was completed) mostly ranges from 800 to 2400 mm/yr (BOM, 2024d). Physiographically the study area largely coincides with the Yilgarn Plateau Province, with only minor overlap onto the Western Coastlands Province of Pain et al. (2011). Topographic altitude ranges from 15 m above sea level (asl) in the southwest (Swan Coastal Plain) to well above 450 m asl in the northwest of the study area (Murchison Plateau). Gnanagooragoo Peak in the Weld Range reaches 737 m asl in the north of the study area. The mean altitude is ~400 m asl (Hutchinson et al., 2008).

The soil types encountered in the study area are, according to the Australian Soil Classification scheme (Isbell et al., 2021; RDA, 2024), most commonly hydrosol (36 % of the sample sites), followed by tenosol (24 %), sodosol (20 %), kandosol (12 %), calcarosol (3.7 %), and the rarer chromosol, kurosol and podosol (each < 2 %). The major river basins that dissect the area are the Salt Lake Basin, which covers almost entirely the eastern half of the study area, whilst the western half comprises from north to south the Gascoyne River, Murchison River, Greenough River, Yarra Yarra Lakes, Ninghan, Moore-Hill Rivers, Avon River, Swan Coast, Murray River (WA), Collie River, Blackwood River, Donnelly River, Warren River, Frankland River and Albany Coast Basins (GA, 1997). Landuse over the area is overwhelmingly 'Grazing native vegetation' (most of the northeastern half of the study area), followed by 'Dryland cropping' (most of the southwestern half of the study area), also known as the wheat belt of Western Australia, with subordinate 'Nature conservation', 'Minimal use', 'Grazing modified pastures', and 'Other protected areas' (ASRIS, 2024).
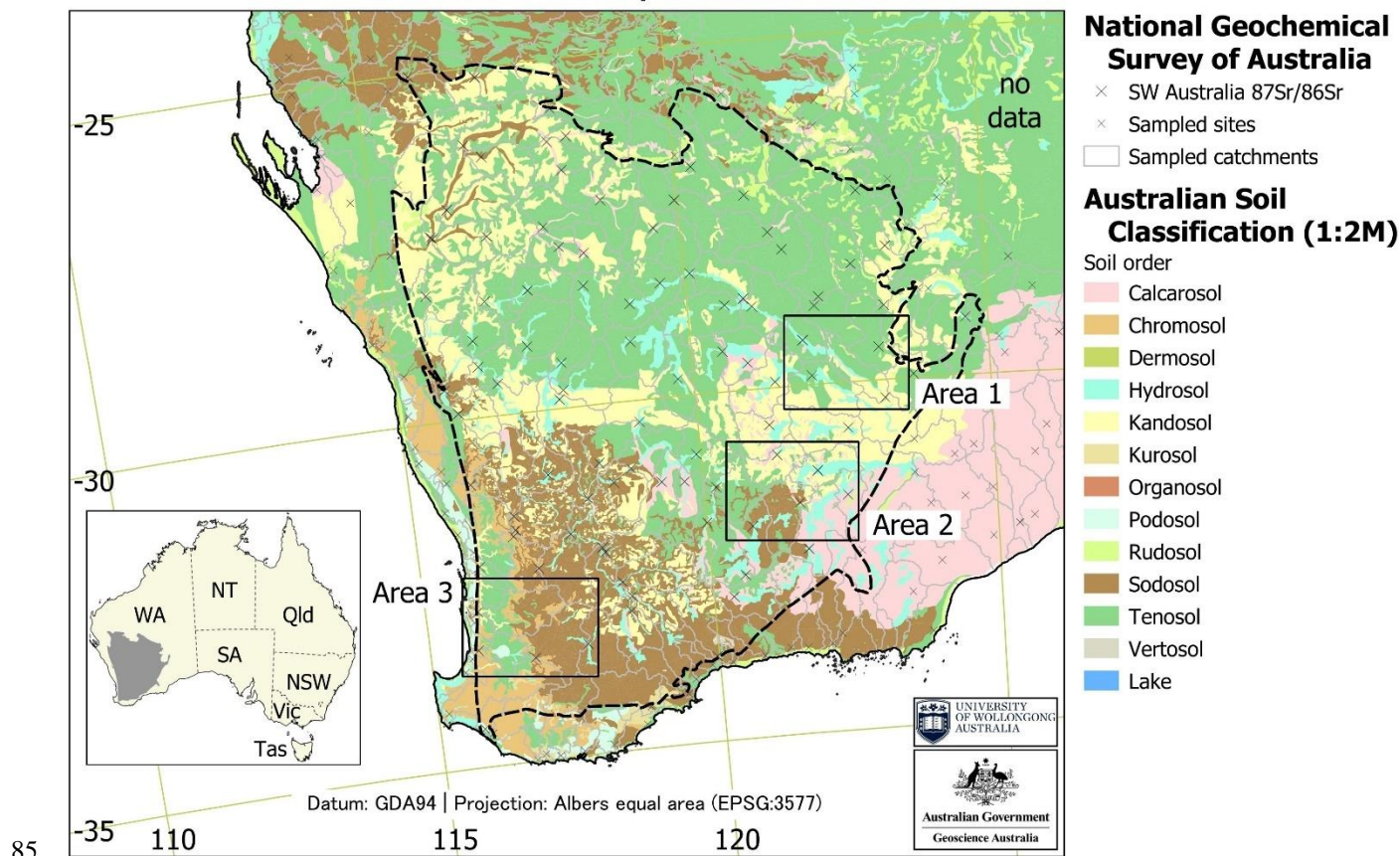
Figure 1. The southwestern Australia Sr isotope study area (see dark grey polygon in inset for location; WA – Western Australia; NT – Northern Territory; Qld – Queensland; NSW – New South Wales; Vic – Victoria; Tas – Tasmania; SA – South Australia), National Geochemical Survey of Australia (NGSA) catchment boundaries (grey polygons), and NGSA ^{87}Sr/^{86}Sr sample locations (grey crosses) overlain on Australian Soil Classification soil orders (Isbell et al., 2021). Other NGSA sample locations (not part of this ^{87}Sr/^{86}Sr study) are shown as smaller light grey crosses. The Yilgarn geological region (Blake and Kilgour, 1998) is outlined in a stippled line. Areas 1, 2 and 3 delineate the locations of Figures S1, S2 and S3 (Supplement), respectively.

The study area focusses on the Yilgarn geological region (Blake and Kilgour, 1998), which comprises rocks dating back to ~3700 million years ago (Ma) and has an extent of ~624 000 km^2. The stratigraphy of the Yilgarn region consists of Archaean sequences (greenstone belts) of fine to coarse clastic sediments, chert, and felsic, mafic and ultramafic volcanics. It also comprises overlying Permian sediments, including coal. Igneous sequences consist of Archaean felsic, mafic and ultramafic volcanics, felsic intrusives, and layered mafic-ultramafic intrusives. Regional metamorphism is low to high grade. Complex folding is recorded in the greenstone belts. At the surface, geology is characterised by low hills, ridges, and breakaways (weathered in-situ rocks); as well as sand plains, salt lakes (commonly underlain by palaeovalleys), and dune fields (transported regolith). The Yilgarn region is extraordinarily endowed in mineral resources, including major gold (Au), nickel (Ni), cobalt

(Co), copper (Cu), silver (Ag), zinc (Zn), lead (Pb), uranium (U), platinum group elements (PGEs), tin (Sn), tungsten (W), molybdenum (Mo), tantalum (Ta), lithium (Li), vanadium (V), titanium (Ti), manganese (Mn), iron (Fe), bauxite, phosphate, and coal deposits (see below).

The main rock types (Blake and Kilgour, 1998) intersected by the NGSA sample sites here are in almost equal proportions 'Meta-igneous felsic intrusive' (39 sites, or 36.4 % of sites) and 'Igneous granitic' (35.5 %), followed by the much less frequent 'Sedimentary siliciclastic' (5.6 %), 'Igneous mafic volcanic' (4.7 %), and in equal proportions 'Igneous felsic volcanic', 'Igneous mafic intrusive' and 'Metasedimentary siliciclastic' (each 3.7 %). Representing 2 % or less each are the 'Meta-igneous mafic volcanic', 'Metamorphic protolith unknown: gneiss', 'Igneous ultramafic volcanic', 'Meta-igneous mafic', and 'Metasedimentary siliciclastic: pelite' rock types.

The bedrock ages (Blake and Kilgour, 1998) intersected at the NGSA sample sites are overwhelmingly Mesoarchaean to Neoarchaean (2960-2650 Ma) (60 sites, or 56 % of sites) and Neoarchaean (2704-2646 Ma) (30 %), followed by the much less frequent Mesoarchaean (2825-2800) (3%). The remaining sites intersect bedrock ranging in age from the Eoarchaean to Neoarchaean (3731-2608 Ma), through Paleoproterozoic (1817-1773 Ma), to Valanginian-Aptian (140-113 Ma) and are represented by only one or two sites (2 % of sites or less) each.

Over 1000 mineral resources or occurrences (mineral deposits + operating mines) are recorded in the Yilgarn geological region (Figure 2; Senior et al., 2021), including:

- 755 'Precious metals – Au, Ag',
- 177 'Battery/alloy metals – Ni, Co, Mn, V, Mo, Mg',
- 47 'Iron ore', 31 'Base metals – Cu (Zn, Pb, Ag, Au)',
- 23 'Uranium',
- 16 'Bauxite', and
- 15 'Base metals – Zn, Pb (Cu, Ag)' occurrences.

Fewer than 10 'Heavy mineral sands', 'Coal', 'Lithium', 'Other metals – Sn, Sb, W, Ta, Nb', 'Light metals – Al, Li, Mg', 'Rare earth elements', 'Fertiliser elements – P, K', 'Platinum group elements', and 'Graphite' occurrences are also reported.

Among all of these, two 'Tier 1' operating mines exist within the Yilgarn region (Senior et al., 2021): Boddington (Au) and Huntly (bauxite) whilst several 'Tier 1' mineral deposits are also present: Earl Grey (Li-Ta-Nb), Mount Mulgine (W), Cawse and Mount Margaret (Ni-Co,) and Honeymoon Well and Yakabindie (Ni) deposits. Cutoff production or resource values for various 'Tiers' are given in Senior et al. (2021). Figure S4 in the Supplement shows the location of the above occurrences.
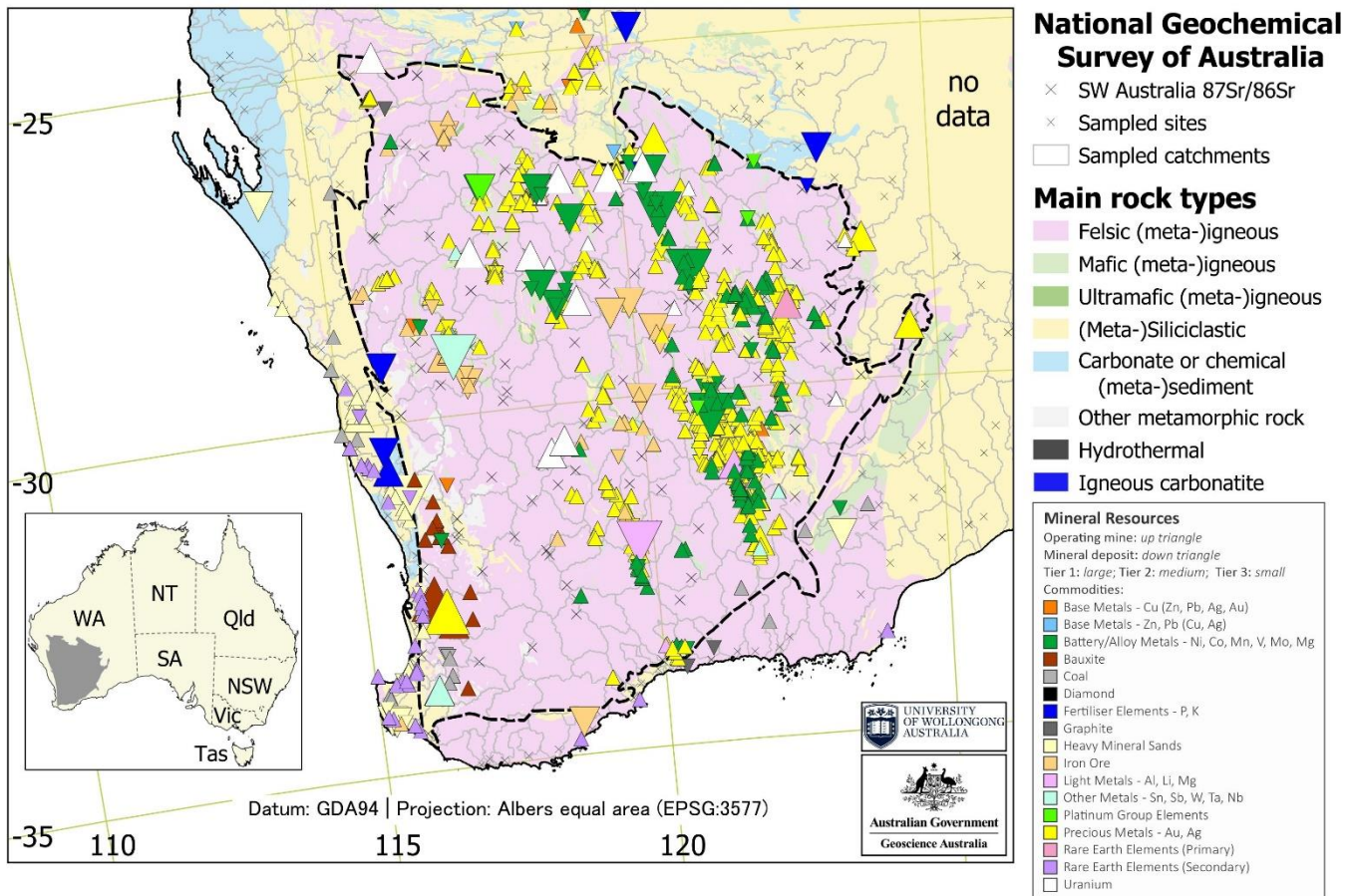
Figure 2. The southwestern Australia Sr isotope study area and National Geochemical Survey of Australia (NGSA) ^{87}Sr/^{86}Sr sample locations (grey crosses) shown with simplified main rock types (Cutten and Riganti, 2020) and mineral resources (Senior et al., 2021). The Yilgarn geological region (Blake and Kilgour, 1998) is outlined in a stippled line.

3 Material and methods

3.1 Material

This study makes use of archive 'catchment outlet sediment' samples collected during the National Geochemical Survey of Australia (NGSA), which covered ~80 % of Australia (de Caritat and Cooper, 2011a, 2016; de Caritat, 2022). The sampling philosophy of the NGSA was to collect naturally mixed and fine-grained fluvial/alluvial sediments from large catchments, thereby obtaining a representative average of the main soil and rock types contributing sediment through weathering. This allowed an ultralow sampling density (~1 sample per 5200 km^2) still being representative of large-scale natural variations (de Caritat and Cooper, 2011b). Sampling floodplain sediments for large-scale, low-density geochemical mapping is a well-established strategy elsewhere, e.g. in Europe (Ottesen et al., 1989; Bølviken et al., 2004). Catchment outlet sediments are

similar to floodplain sediments in the sense that they are deposited during receding floodwaters outside the riverbanks, but with the added complexity that, in Australia, many areas can also experience addition (or loss) of material through aeolian

145 processes. The sampled floodplain geomorphological entities are typically vegetated and biologically active (plants, worms, ants, etc.) thereby making the collected materials true soils, albeit soils developed on transported alluvium parent material.

The sampling medium and density were both strategically chosen in the NGSA project to prioritize coverage over resolution. This was justified by the fact that the NGSA was Australia's first and, to-date, only fully integrated, internally consistent geochemical survey with a truly national scope. In terms of the present study area, it is clear that these choices have implications

150 on the granularity of the patterns revealed by the Sr isoscape; as the collection of Sr isotope data in Australia using NGSA samples grows in the future (e.g. de Caritat et al., 2022, 2023, and this contribution), it is hoped the value of coverage will prevail over a relative low resolution of detailed features.

The NGSA collected samples at two depths, a 'top outlet sediment' (TOS) from a shallow (0.1 m) soil pit approximately 0.8 m x 0.8 m in area, and a 'bottom outlet sediment' (BOS) from a minimum of three auger holes generally drilled within ~10 m

155 of the TOS pit. The auger holes were drilled as deep as possible (to refusal or to maximum depth of 1 m), and the BOS sample was collected on average from a depth of 0.6 m to 0.8 m from all augered holes. A field manual was compiled to record all sample collection method details, including site selection (Lech et al., 2007). Sampling for the NGSA took place between July 2007 and November 2009, and the field data were recorded in Cooper et al. (2010). In the laboratory, the samples were air dried at 40 °C for a minimum of 48 h (or to constant mass) before being further prepared (see de Caritat et al., 2009) for the

160 comprehensive geochemical analysis program of the NGSA (see de Caritat et al., 2010). For Sr isotope analysis, an aliquot of minimum ~1 g of sample milled to a fine powder using a carbon steel ring mill was retrieved. The main sample type selected for the present Sr isotope study was NGSA BOS < 2 mm in order to be as representative as possible of the geogenic background unaffected by modern landuse practices and inputs (e.g. fertilizers). A few NGSA TOS < 2 mm samples, prepared in an identical fashion, were also analysed.

165 Overall 107 NGSA BOS < 2 mm and 13 NGSA TOS < 2 mm were analysed for Sr isotopes as detailed in the Methods below (Sect. 3.2), for a total of 120 analyses. Given that there are ~10 % field duplicates in the NGSA, all those samples originate from within 97 NGSA catchments, which together cover 533 000 km^2 of southwestern Australia (see Figure 1).

3.2 Methods

Samples were prepared and analysed for Sr isotopes (^{87}Sr/^{86}Sr) at the Wollongong Isotope Geochronology Laboratory (WIGL).

170 Approximately 50 mg of sample was weighed and digested in a 2:1 mixture of hydrofluoric and nitric acids. All reagents used were Seastar Baseline® grade, with Sr concentrations typically < 10 parts per trillion. Following digestion, samples were re-dissolved in aqua regia (twice if needed) in order to eliminate any fluorides, followed by nitric acid twice. Finally, samples were re-dissolved in 2 M nitric acid prior to ion exchange chromatography. Strontium was isolated from the sample matrix

using automated, low-pressure chromatographic system Elemental Scientific prepFAST-MC™ and a 1 mL Sr–Ca column
(Eichrom™) (Romaniello et al., 2015). The Sr elutions were re-dissolved in 0.3 M nitric acid.

Strontium isotope analysis was performed on a Thermo Scientific Neptune Plus multicollector-inductively coupled plasma-mass spectrometer (MC-ICP-MS) at WIGL. The sample introduction system consists of an ESI Apex-ST PFA MicroFlow nebulizer with an uptake rate of ~0.1 mL min^{-1}, an SSI Quartz dual cyclonic spray chamber, jet sample, and X-skimmer cones. Measurements were performed in low-resolution mode. The instrument was tuned at the start of each session with a 20 parts per billion Sr solution, and sensitivity for ^{88}Sr was typically around 4 V. Masses 88, 87, 86, 85, 84, and 83 were collected on Faraday cups. Rubidium removal during chromatography was assessed by determining the amounts of Rb before and after chromatography. Before chromatography, an aliquot of solution prepared for chromatography was taken and diluted 100 times in 0.3 M nitric acid. This solution was analysed for Rb and Sr concentrations by quadrupole ICP-MS at WIGL. To determine the amount of Rb after chromatography, the Rb concentration was determined during Sr isotopic analysis by using (i) the Sr sensitivity for the session in question and (ii) the measured ^{85}Rb/^{88}Sr ratio. Instrumental mass bias was internally corrected using measured ^{87}Sr/^{86}Sr. Masses 85 and 83 were used to correct for the isobaric interference of ^{87}Rb and ^{86}Kr, respectively.

3.3 Quality Assessment

National Institute of Standards and Technology (NIST) strontium carbonate isotope Standard Reference Material SRM987 was used as a secondary standard and measured after every five samples to assess accuracy during analysis. Accuracy of the whole procedure was assessed by processing United States Geological Survey (USGS) reference material Basalt from the Columbia River standard BCR-2 (Plumlee, 1998). The mean ± 2se ^{87}Sr/^{86}Sr for BCR-2 in this study is 0.704998 ± 14 ($n = 4$), within error of the value in Jweda et al. (2016) (0.704500 ± 11). Total procedure blanks ranged between 0.037 and 0.109 ng Sr ($n = 4$). Ten field duplicate sample pairs (collected at a median distance of ~80 m from one another on the same landscape unit, see Lech et al., 2007) were analysed for ^{87}Sr/^{86}Sr in the BOS < 2 mm sample, and returned a median relative standard deviation of 1.76 %. The relative standard deviation from field duplicates includes natural variability (mineralogical/chemical heterogeneity of the alluvial deposit), as well as sample collection, preparation, and analysis uncertainties.

It was assessed whether high ^{87}Sr/^{86}Sr ratios (> 0.8) were an analytical artefact since incomplete removal of Rb and the isobaric interference of ^{87}Rb on ^{87}Sr can result in inaccurately high ^{87}Sr/^{86}Sr ratios. Rubidium removal was generally better than 99.995 % and there was no relationship between Rb removal and measured ^{87}Sr/^{86}Sr ratios (incomplete Rb removal should produce an inverse relationship between Rb removal and ^{87}Sr/^{86}Sr ratios). Thus, we are confident that the high ^{87}Sr/^{86}Sr ratios measured are accurate.

Overall, we feel that the quality of the ^{87}Sr/^{86}Sr data presented herein is adequate for the purpose of regional mapping, and that reporting ^{87}Sr/^{86}Sr data to the third decimal place with an indicative fourth decimal place is appropriate for this work. This relatively low precision obtained for field duplicates is attributed to heterogeneity of the alluvial deposits, since precision relating to sample preparation and analysis for Sr isotopes is at the fifth decimal place (see results for BCR-2 above).

3.4 Data Analysis

Data management, graphing and visualisation were performed using Microsoft Excel® and the Statistics Kingdom online graphing tools (https://www.statskingdom.com/). Maps were prepared using the open software QGis (version 3.28.12–Firenze). Symbology for displaying $^{87}Sr/^{86}Sr$ data here was either point-based at the sampling site, catchment-based attributing the $^{87}Sr/^{86}Sr$ value and colouring to the whole catchment, or as an interpolated continuous grid. In either case, the data were classified in eight equal quantile classes (12.5 % of the data each). The colour ramp used was 'Roma', a colour vision deficiency (CVD) friendly colour gradient (Crameri, 2018; Crameri et al., 2020). The catchment-based representation is appropriate for the sampling medium used, catchment outlet sediment, which is thought to be representative of the average materials in the catchment (see Sect. 3.1). For this display mode, multiple $^{87}Sr/^{86}Sr$ values within any catchment (e.g. field duplicates) were averaged to a single value per catchment. Interpolation was performed in QGis using inverse distance weighting with a power of two and a spatial resolution of 0.25 degree. All maps are shown in Albers equal area projection.

4 Results

The 107 NGSA BOS < 2 mm $^{87}Sr/^{86}Sr$ values reported herein range from 0.7152 to 1.0909 (range = 0.3757). The median is 0.7560 and the mean 0.7691 (standard deviation = 0.0521; kurtosis = 14.4; skewness = 3.1). Figure 3 illustrates the univariate structure of the new data, which can be described as asymmetrical (right/positive skewed) and leptokurtic (long heavy tail). Six values at 0.8500 (upper whisker) and above can be described as Tukey outliers (Tukey, 1977).
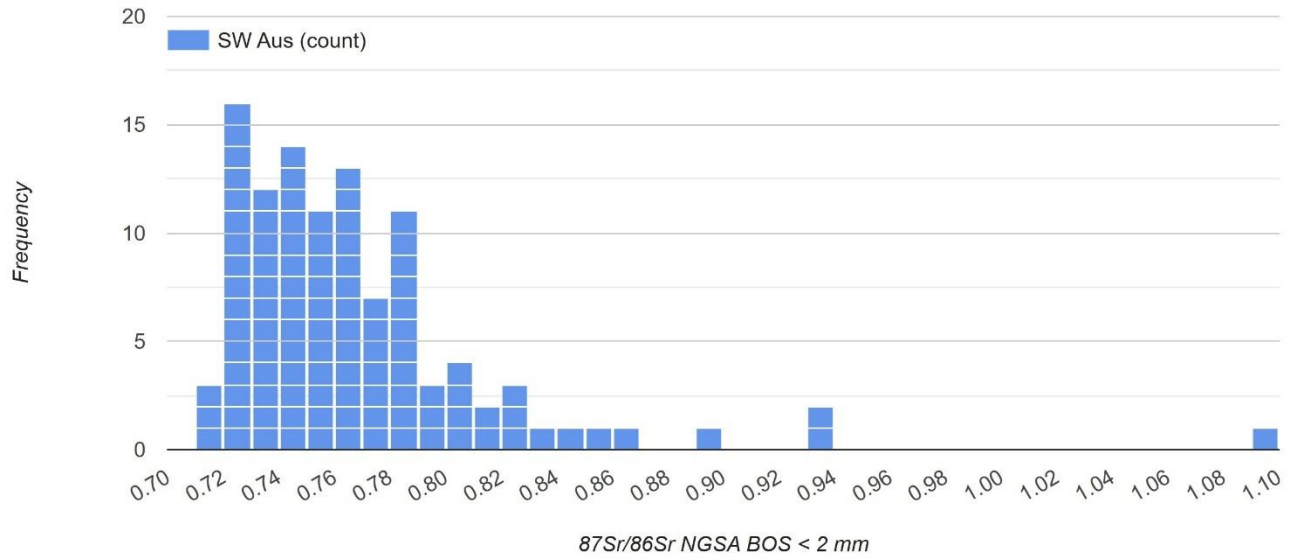
Figure 3. Histogram of the ^{87}Sr/^{86}Sr data ($n = 107$) from the southwestern Australia Sr isotope study area. Sample medium is the < 2 mm fraction of NGSA Bottom Outlet Sediment (BOS).

Spatially, the ^{87}Sr/^{86}Sr values define large-scale, coherent patterns with multi-point high and low regions (Figure 4). The main high (radiogenic) ^{87}Sr/^{86}Sr values form a north-south trending elongated area across the central/western part of the Yilgarn geological region. Prominent low (unradiogenic) ^{87}Sr/^{86}Sr values define a large area along the southeastern margin of the Yilgarn. In Sect. 5, these patterns are compared to existing knowledge of rock isotopic compositions, as a validation of the present results.

a)

Strontium Isoscape of Southwestern Australia
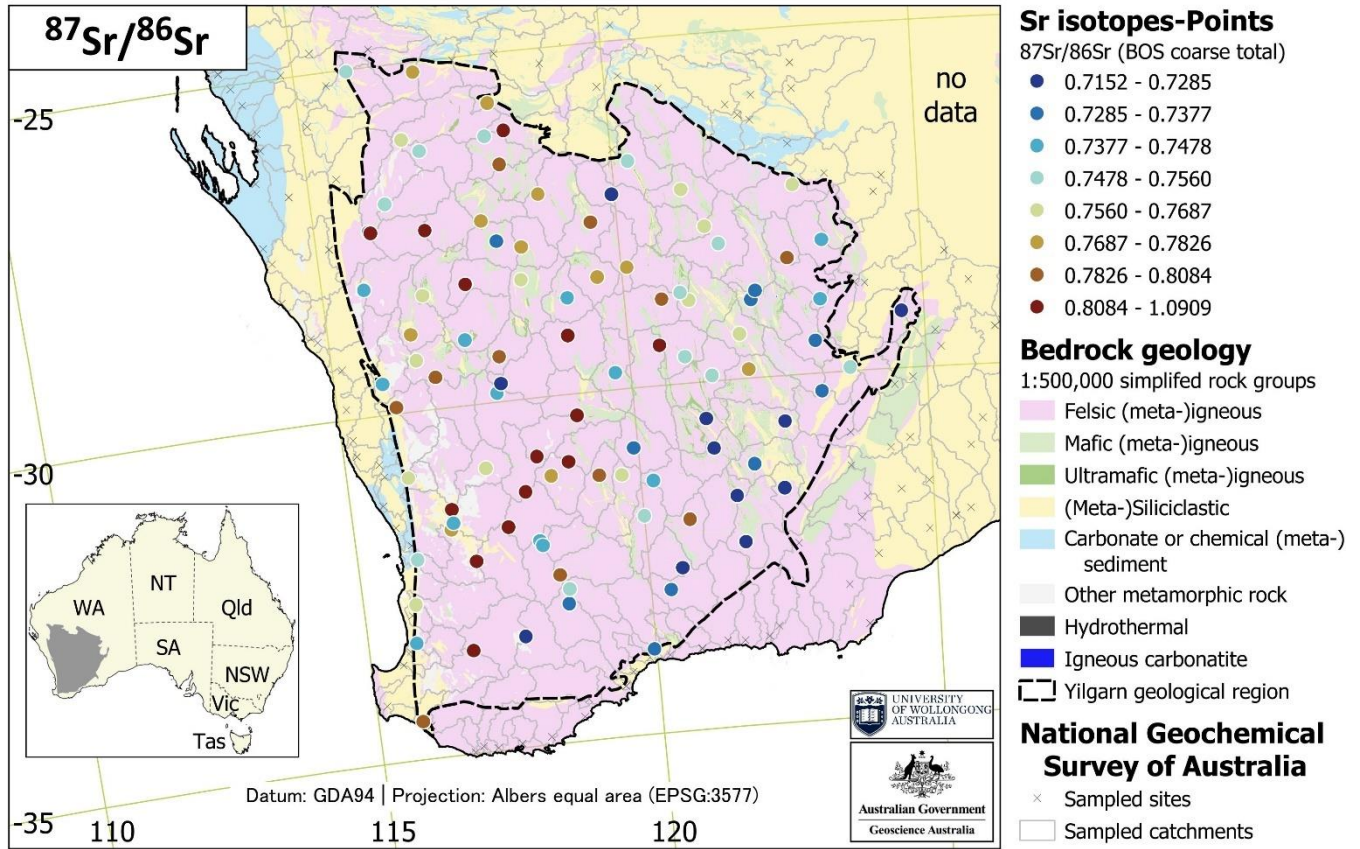
c)
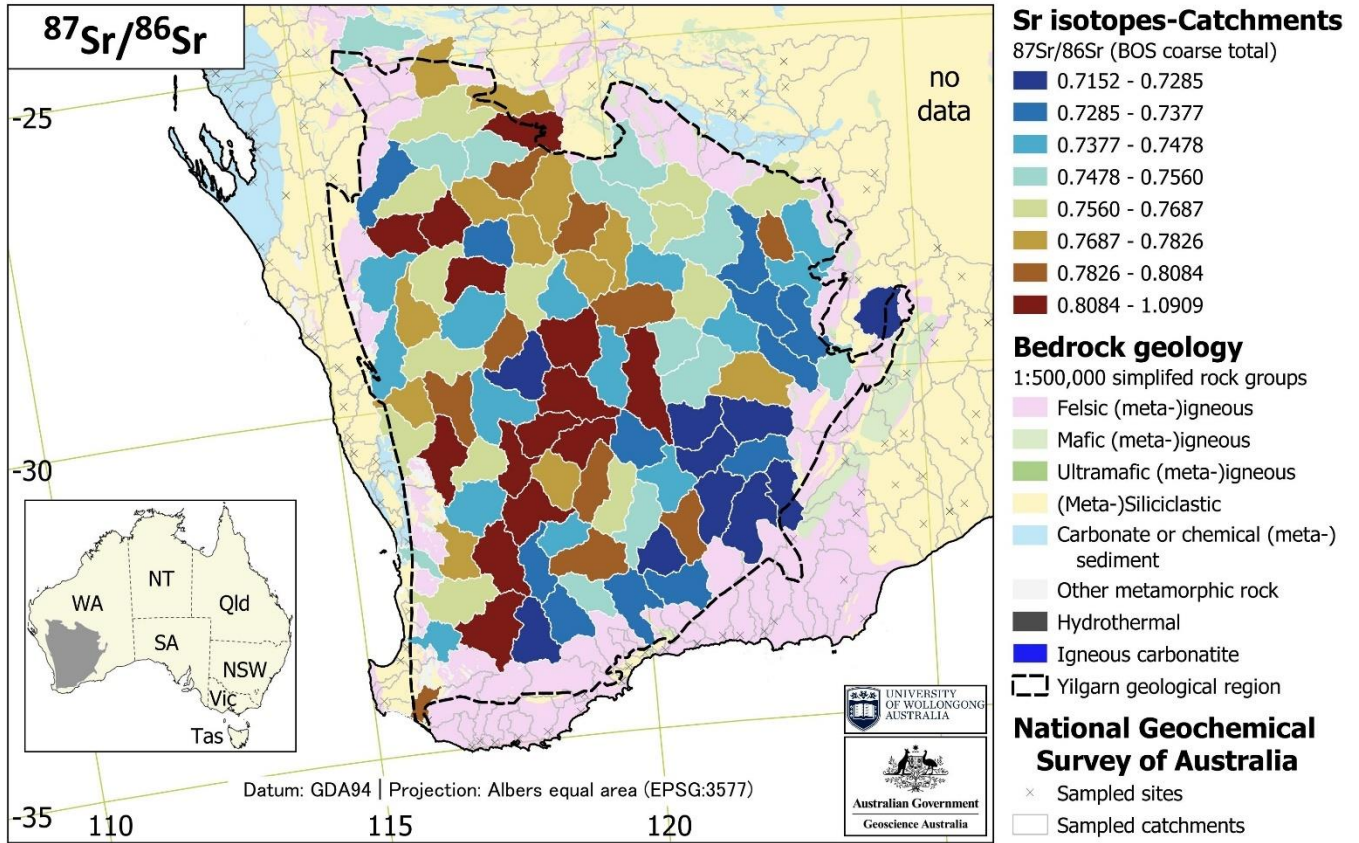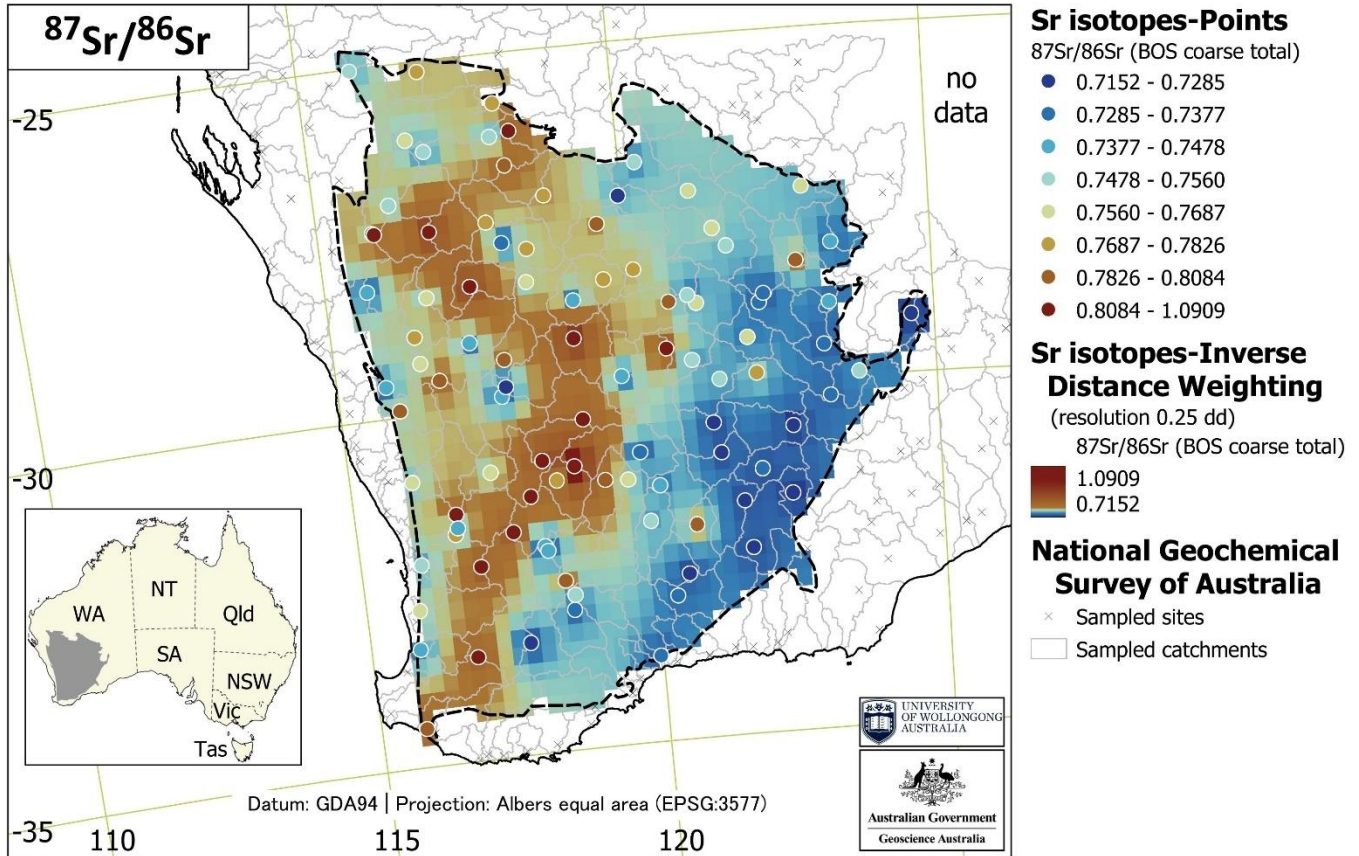
235 **Figure 4. The southwestern Australia Sr isotope study results shown as a dot map (a), a catchment-averaged map (b) both overlain on a simplified main rock types (Cutten and Riganti, 2020), and as an interpolated grid map (c). Interpolation was performed using inverse distance weighting with a power of two and a spatial resolution of 0.25 degree. The Yilgarn geological region (Blake and Kilgour, 1998) is outlined in a stippled line.**

5 Discussion

240 ### 5.1 Validation against bedrock datasets

A comparison of the present results with selected rock $^{87}Sr/^{86}Sr$ datasets from previous work in the Yilgarn region indicates a good correspondence between our bottom of catchment sediment $^{87}Sr/^{86}Sr$ and outcropping or subcropping rocks within their upstream catchment (see Supplement). For instance, in Area 1 (see Fig. 1 and Fig. S1 in Supplement) our relatively unradiogenic catchment sediment $^{87}Sr/^{86}Sr$ value of 0.7347 is intermediate between the values of 0.7265 and 0.7416 reported

245 for two gneiss samples from the Kirgella rock-hole by McCulloch et al. (1983).

In Area 2 (see Fig. 1 and Fig. S2 in Supplement) another also relatively unradiogenic catchment sediment value of 0.7235 is only marginally larger than a gneiss value (0.7207) from Pioneer Dome reported by McCulloch et al. (1983). In another catchment within Area 2, our $^{87}Sr/^{86}Sr$ value of 0.7255 is again only slightly above the values reported by McCulloch et al. (1983) for two gneiss samples from Connolly Siding (0.7195 and 0.7234).

250 In Area 3 (see Fig. 1 and Fig. S3 in Supplement) we validate some of the more radiogenic $^{87}Sr/^{86}Sr$ values of our work. In the central catchment of Area 3 our sediment $^{87}Sr/^{86}Sr$ value is 0.7671. This catchment contains 14 whole-rock analyses of agmatitic gneiss, gneiss, gneissic granite, granite, and porphyritic granite samples from the Harvey-Mount Saddleback region reported by De Laeter and Libby (1993) to range in $^{87}Sr/^{86}Sr$ from 0.7064 to 1.0847 (average 0.7875). Ignoring the extreme outlier value of 1.0847 from a porphyritic granite, the range reduces to 0.7064 - 0.8212 and the average to 0.7646, only slightly

255 below our NGSA based result. Sediment from the catchment immediately to the southeast of that one (see Fig. S3 in Supplement) returned a radiogenic $^{87}Sr/^{86}Sr$ value of 0.8225. Four whole-rock samples of granite and one of porphyritic granite reported by De Laeter and Libby (1993) range from 0.7618 to 0.9188, averaging 0.7986, a relatively radiogenic value. We acknowledge that the above comparison of sediment isotopic signatures with whole-rock data has limitations, including the small number of primary $^{87}Sr/^{86}Sr$ data and the fact that we cannot weigh those values to account for how representative a

260 particular lithology is of the area or how weatherable it is. Despite this, the first-order validation above suggests that the Sr isotopic signature obtained on NGSA catchment sediments is in overall agreement with observed whole-rock data.

5.2 Relationship to bedrock lithology and age

In order to investigate the influence of lithology and age on the $^{87}Sr/^{86}Sr$ values, we intersected each sample site with the 1:500 000 interpreted geology layer (Cutten and Riganti, 2020). In this fashion we were able to assign a major lithology and age

265 bracket to each $^{87}Sr/^{86}Sr$ datapoint. To simplify interpretation, we grouped the lithologies into three classes: 1) granites, 2) mafic and ultramafic, and 3) other lithologies. Similarly, for each age bracket (age from, age to) in the database, we calculated the mean age as the average of minimum age and maximum age. In Figure 5, we show the results of this classification as a boxplot of $^{87}Sr/^{86}Sr$ values vs lithology groups (Fig. 5a) and as a scatter plot of $^{87}Sr/^{86}Sr$ values vs age (Fig. 5b). From these plots, it is possible to say that the granites predictably tend to have higher $^{87}Sr/^{86}Sr$ values than the (ultra-)mafic lithologies

270 (other than minimum values, all boxplot metrics, including median, 75th percentile, upper fence, and maximum are higher). The trend of $^{87}Sr/^{86}Sr$ values with age is more nuanced, with less radiogenic $^{87}Sr/^{86}Sr$ values (say, lower than 0.81) observed in all age groups from 3731 Ma to 126 Ma (Fig. 5b). However, all $^{87}Sr/^{86}Sr$ values greater than 0.81 exclusively originate from rocks older than 2600 Ma. These older rocks are all granitic, except in two instances. All the (ultra-)mafic rocks, which are also in the age bracket 3300-2600 Ma, have $^{87}Sr/^{86}Sr$ values below 0.8. All the rocks younger than 2500 Ma have $^{87}Sr/^{86}Sr$

275 values below 0.81 and are all lithologically neither granites nor (ultra-)mafic rocks. A caveat to the above interpretation is that our NGSA samples were not exclusively from the interpreted basement rock type beneath their location but also integrate contributions from other lithologies higher up within their catchment. Nonetheless, the observed relationships between

^{87}Sr/^{86}Sr values, lithology and age are consistent with the controls on ^{87}Sr/^{86}Sr values (e.g., Rb content in felsic rocks and time for ^{87}Rb to decay to ^{87}Sr).
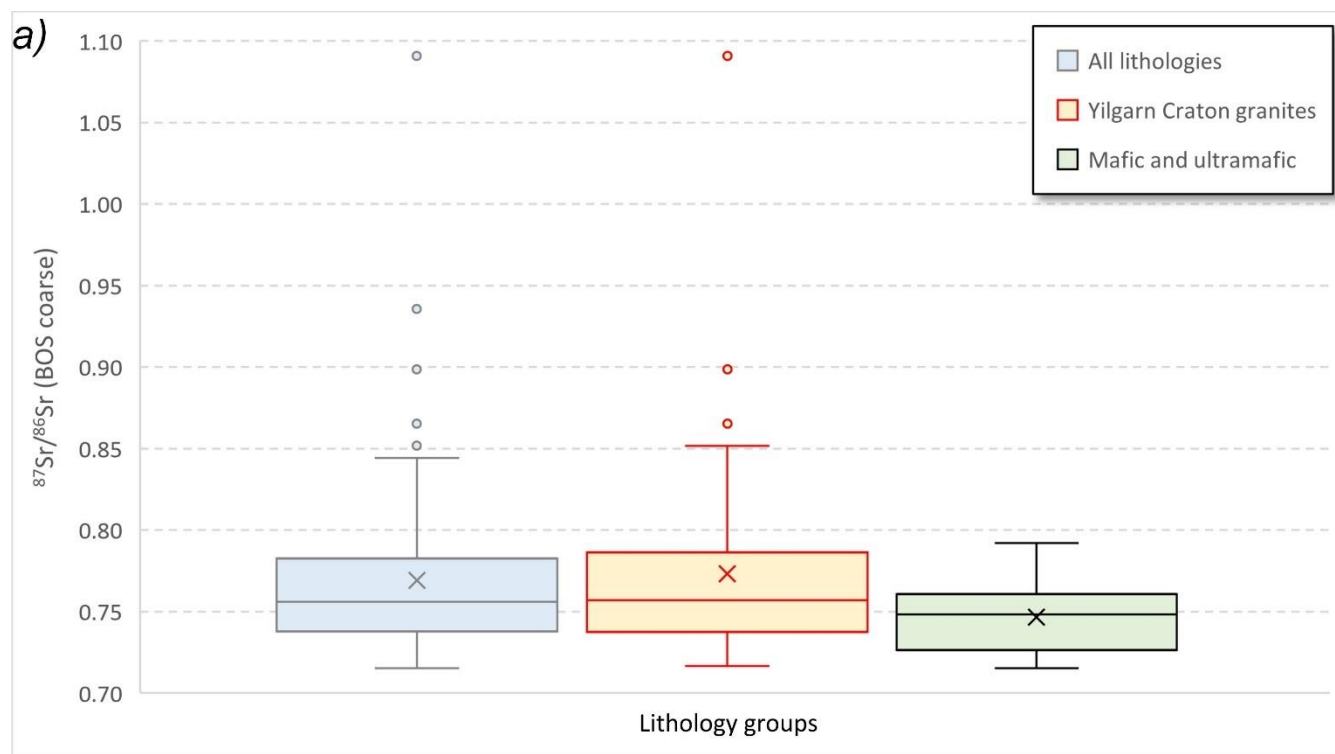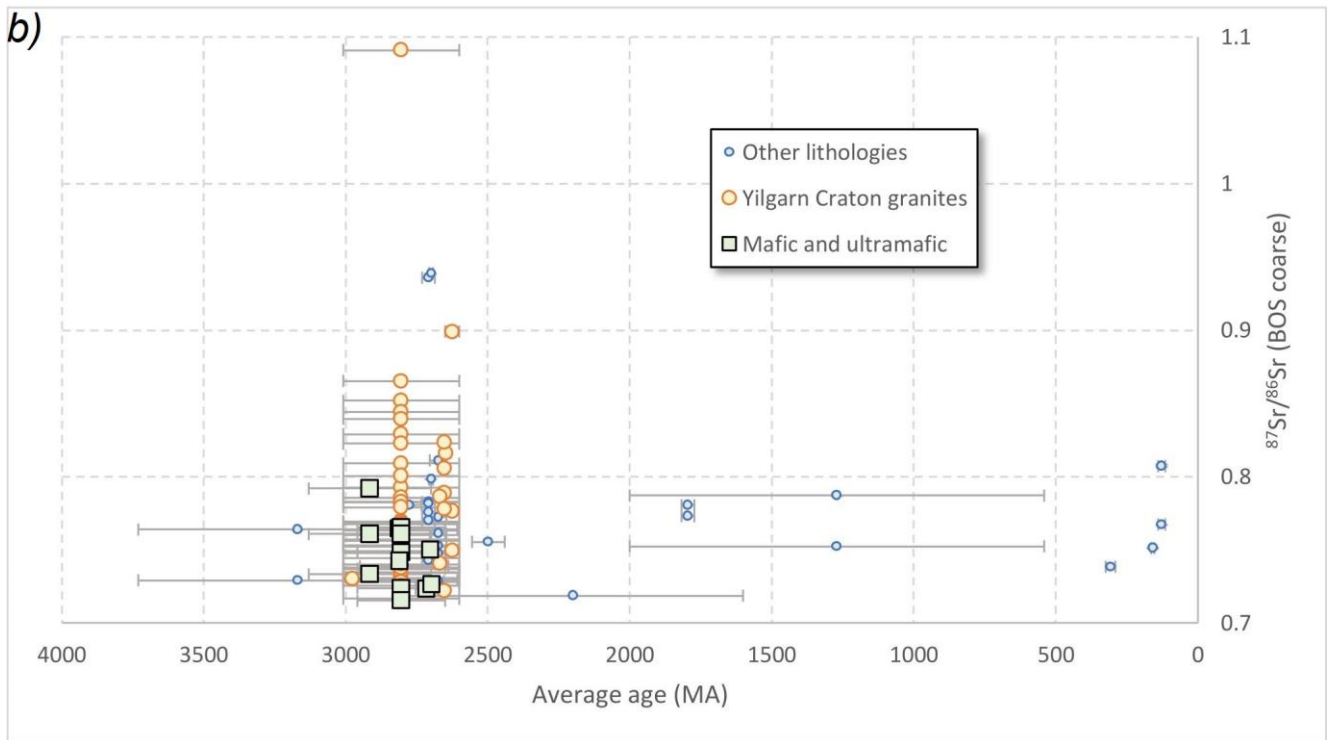
Figure 5. The southwestern Australia Sr isotope study results sub-grouped by major lithology type (a) and average age (b). Population sizes (*n*) are 107 for All lithologies, 61 for Yilgarn Craton granites, 13 for Mafic and ultramafic, and 33 for Other lithologies. Average ages in (b) are shown as symbols with bars stretching to reported minimum and maximum age for each rock unit.

5.3 Relationship to mineralisation

De Caritat et al. (2023) found a tantalizing relationship between $^{87}Sr/^{86}Sr$ values in catchment sediments from northern Australia and operating mines and/or mineral deposits within their catchment. In order to investigate this further in southwestern Australia, we associated all the operating mines and mineral deposits from the AIMR report (Senior et al., 2021) with the relevant $^{87}Sr/^{86}Sr$ data point from the outlet of each catchment. Thus, each $^{87}Sr/^{86}Sr$ value in our dataset may be associated with none, one, or several mineral occurrences in their catchment.

In Figure 6, we plot the $^{87}Sr/^{86}Sr$ values associated with each major commodity group. Whilst over half of the ca 1000 mineral occurrences in the region originate from catchments with an intermediate $^{87}Sr/^{86}Sr$ signature (0.728 – 0.767), several occurrences are associated with higher values ($^{87}Sr/^{86}Sr > 0.8$). The very highest $^{87}Sr/^{86}Sr$ value in the Yilgarn dataset (1.0909) comes from a catchment that contains known Co, Ni, Au and Fe ore deposits. All the outlier $^{87}Sr/^{86}Sr$ values per commodity group are labelled in Figure 6 and attributed to the known mineral occurrence (i.e. mineral deposit or operating mine) found in their catchment. Figure S4 in the Supplement shows maps of where these labelled mineral occurrences are located. About 40 mineral occurrences are found in catchments that have positive outlier $^{87}Sr/^{86}Sr$ values for at least one major commodity group; only three are associated with negative outlier values.

The major, 'Tier 1' operating Au mine (Boddington) in the Yilgarn region is in a catchment with outlet sediment $^{87}Sr/^{86}Sr$ signatures of 0.7671 (within the fourth quartile of the relevant commodity group). The 'Tier 1' mineral deposits of Earl Grey (Li-Ta-Nb) has a $^{87}Sr/^{86}Sr$ catchment isotope signature of 0.7521 (second quartile), Mount Mulgine (W) 0.7675 (fourth quartile), Cawse (Ni-Co) 0.7232 (first quartile), Mount Margaret (Ni-Co) 0.7375 (second quartile) and 0.7489 (third quartile), Honeymoon Well (Ni) 0.7483 (third quartile), and Yakabindie (Ni) 0.7222 (first quartile) and 0.7886 (fourth quartile). Some of these are above the total project median value of 0.7560.

We conclude that the relationship between catchment sediment $^{87}Sr/^{86}Sr$ signature and mineral resources within the catchment is complex and probably influenced by many factors. These will likely include proximity of sampling site to resource, nature of the host lithology to the resources (rock type, degree of alteration and weathering, depth, fracturing, etc.), and geological heterogeneity of the catchment, among others. This relationship and thus the potential to use $^{87}Sr/^{86}Sr$ as tool in mineral prospectivity analysis, however, deserves deeper investigation beyond the scope of the present paper.
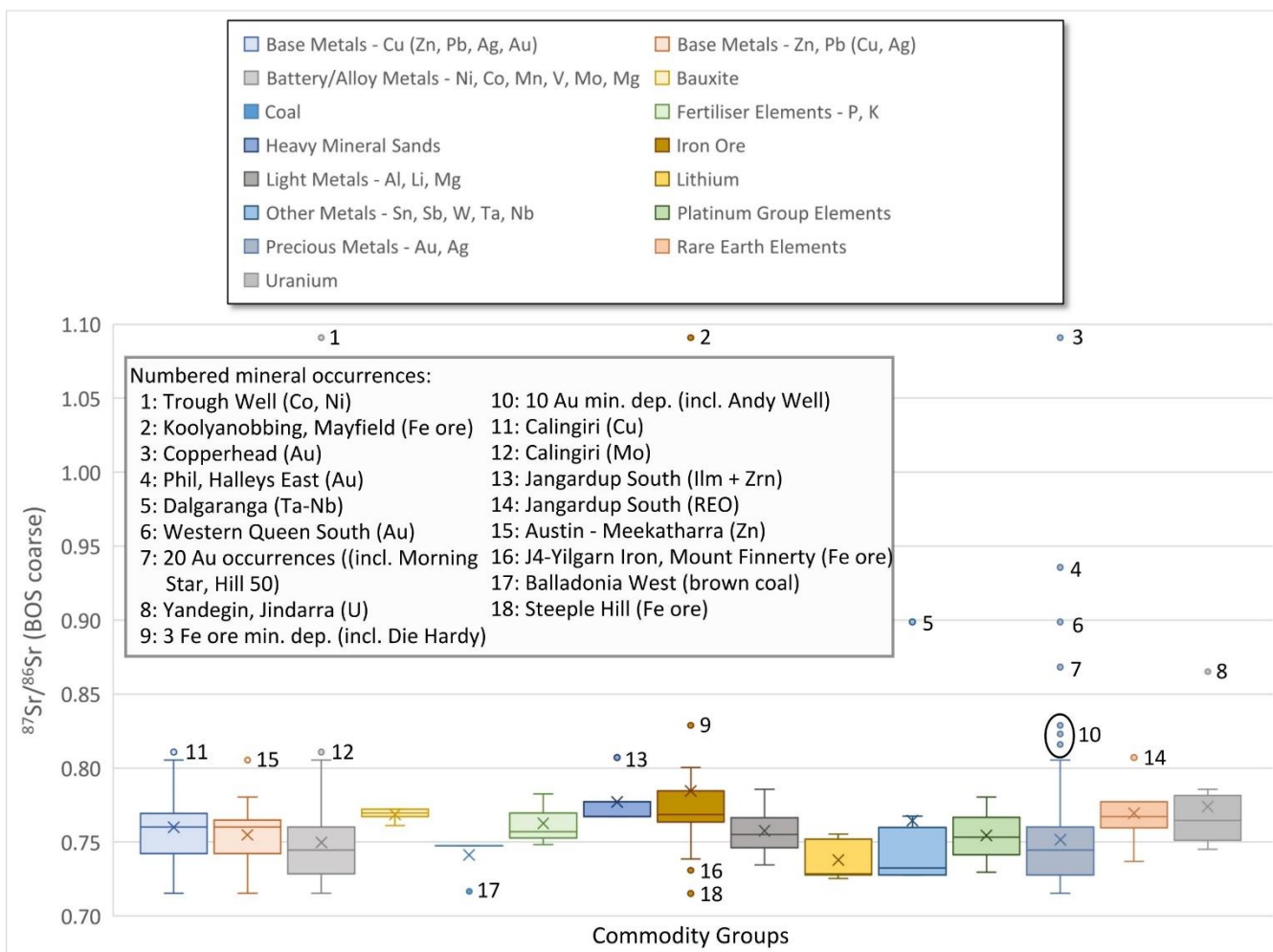
Figure 6. The southwestern Australia Sr isotope study results shown as boxplots sub-grouped by major commodity groups. Any sediment ^{87}Sr/^{86}Sr value associated with a catchment hosting one or more reported mineral resource(s) (Senior et al., 2021) is attributed to the relevant commodity group(s), and may thus appear in more than one boxplot. All outlying mineral resources are labelled. Figure S4 in the Supplement shows the location of selected mineral deposits and operating mines.

5.4 Comparison with previous NGSA Sr isotope dataset

In previous reports, we presented new ^{87}Sr/^{86}Sr data also using NGSA sediment samples over large areas of Australia (de Caritat et al., 2022, 2023). These results are summarised in Table 1 and compared with the present dataset. Overall, there are now 576 internally consistent ^{87}Sr/^{86}Sr values from large Australian catchments covering in excess of 2 500 000 km^2 across a range of topographic, climatic, landuse, lithological and rock-age conditions (environmental diversity). From this compilation, it can be seen that the lowest minimum ^{87}Sr/^{86}Sr value (0.7048) came from the northern Australia subset, the lowest median (0.7199) came from the southeastern Australia subset, and both the highest median (0.7560) and maximum (1.0909) from the southwestern Australia subset. The smallest range came from southeastern Australia (0.0422), whereas the largest (0.3757) came from southwestern Australia. This in part reflects the size of the areas, both in terms of geographical size and sample size, in part the more homogeneous lithological types and rock-age ranges found in the southeastern Australia study area. Overall, there is reason to believe that the compilation of 576 new ^{87}Sr/^{86}Sr data points representing over 2 500 000 km^2 of diverse geological terrain is appropriate for a representation of the isotopic makeup of the upper continental crust, which will be reported on separately.

Table 1. Comparison of ^{87}Sr/^{86}Sr data from this study with the other two large-scale studies (Caritat et al., 2022, 2023) and preliminary national strontium isoscape for Australia (count, minimum, median, mean, standard deviation of the sample, maximum, range, and upper whisker for Tukey outlier detection). All sample types are NGSA BOS coarse, i.e. subsoil (on alluvium), < 2 mm fraction. All samples were milled then digested using HF-HNO$_3$-AR; Sr was separated by ion chromatography prior to isotopic analysis by MC-ICP-MS (see Sect. 3).

Area	Size (km^2)	n	Min	Med	Mean	SD	Max	Range	Upper whisker	Source
Southwestern Australia	533 000	107	0.7152	0.7560	0.7691	0.0521	1.0909	0.3757	0.8500	This study
Northern Australia	1 536 000	357	0.7048	0.7406	0.7532	0.0480	1.0330	0.3282	0.8383	de Caritat et al., 2023
Southeastern Australia	529 000	112	0.7089	0.7199	0.7220	0.0106	0.7511	0.0422	0.7491	de Caritat et al., 2022
Preliminary national isoscape	2 598 000	576	0.7048	0.7377	0.7501	0.0467	1.0909	0.3861	0.8314	All above sources

5.5 Toward a national Sr isoscape

The internal consistency, environmental diversity, and geographical and statistical extent of the compilation of large-scale ^{87}Sr/^{86}Sr datasets (de Caritat et al., 2022, 2023, and this study) discussed above allow for their preliminary integration and

340   consideration of progress toward a national Sr isoscape. In Figure 7, we show the national compilation of the above three large-scale Sr isotope study areas into a single isoscape with a unified classification and colour legend.

It shows for the first time how the southeastern region is overwhelmingly relatively unradiogenic (^{87}Sr/^{86}Sr < 0.7376), with the Broken Hill region in the centre and the Shepparton region in the far southeast standing out as moderately radiogenic (^{87}Sr/^{86}Sr 0.7376 – 0.7642) compared to the local background. In northern Australia, the Barkly Tableland in the Northern

345   Territory and the southern Cape York peninsula in Queensland have an unradiogenic background of similar magnitude to the southeastern Australia area (^{87}Sr/^{86}Sr < 0.7376). Much of the Cape York Peninsula has more radiogenic ^{87}Sr/^{86}Sr values (0.7376 – 0.7890), whilst the regions flanking the Barkly Tableland on the eastern, northern and western sides (including Mount Isa, Macarthur River, Alligator River, and Tanami Desert-Reynolds Range area in the Northern Territory) have moderate to extreme radiogenic ^{87}Sr/^{86}Sr values (0.7376 – 1.0909). Also in that category are the King Leopold Ranges-Napier Range and

350   the Nullagine River (Pilbara) areas in northwestern Western Australia. The Yilgarn Craton, apart from most catchments along its southern and eastern flanks, also falls into the moderate to extreme radiogenic ^{87}Sr/^{86}Sr values (0.7376 – 1.0909) category.
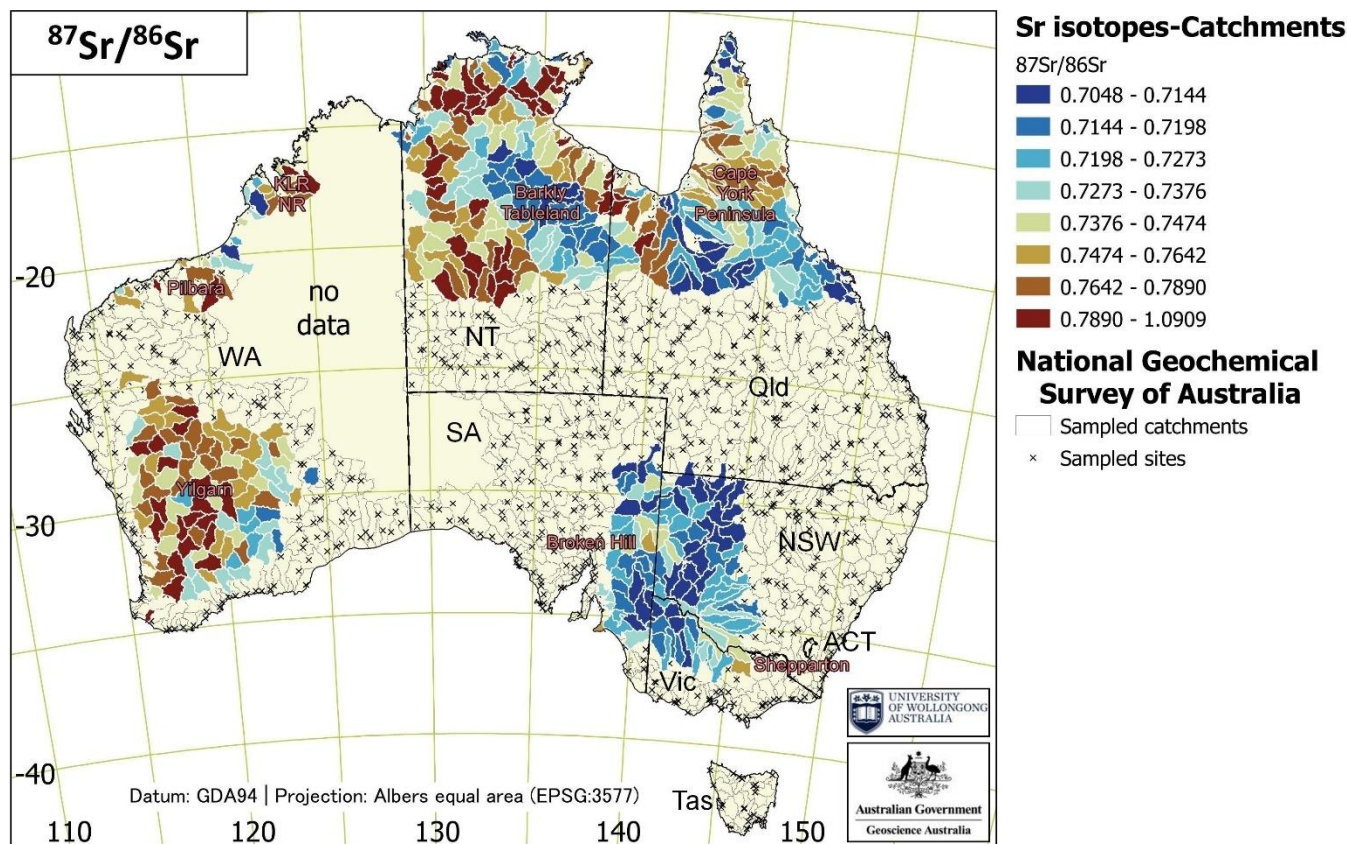
Figure 7. The combined southeastern (de Caritat et al., 2022), northern (de Caritat et al., 2023), and southwestern (this study) Australia Sr isotope areas shown as a single, catchment-averaged Sr isoscape with unified classification and colour legend (WA –
355   **Western Australia; NT – Northern Territory; Qld – Queensland; NSW – New South Wales; ACT – Australian Capital Territory; Vic – Victoria; Tas – Tasmania; SA – South Australia). Localities referred to in the text are labelled in orange (KLR: King Leopold Ranges; NR: Napier Range).**

6 Future work

As the strategy of the NGSA and therefore of the current Sr isoscape roll-out was very much focussed on the large scale rather
360 than the detailed, process-oriented understanding, it would be beneficial to link the two scales by studying a few NGSA catchments in greater detail. The catchments could be selected to represent a range of geological, ecological, topographic and climatic conditions. This could include smaller (nested) catchments, soil profiles and catenas, multi-media (rock, soil, groundwater, plants, organisms), and temporal (seasonal and decadal) studies of Sr isotopes in the Australian context. Machine learning techniques could be applied to the current $^{87}Sr/^{86}Sr$ datasets to learn the complex relationships between this
365 variable and multiple environmental predictors, including geological, climatic, ecological and topographic covariables. Scope also exists for continuing the analysis of the remaining NGSA samples (approximately 700 additional samples), which would deliver a Sr isoscape covering ~80 % of Australia. This could involve other laboratories for the isotopic analysis and could be used as a testbed to establish a multi-institutional, national infrastructure for excellence in isotopic analysis in Australia. Another possible avenue of progressing a national isotopic coverage would be to analyse $^{87}Sr/^{86}Sr$ in the NGSA samples for
370 labile Sr as a proxy for bioavailable Sr. Such results could readily be applied to numerous archaeological, forensic and environmental questions with uses beyond the classical geosciences, which was the primary motivation of the initial Sr isoscape work.

7 Data availability

The new spatial Sr isotope dataset for the southwestern Australia region is publicly available from
375 https://dx.doi.org/10.26186/149755 (de Caritat et al., 2024).

8 Conclusions

One hundred and twenty new strontium (Sr) isotopic compositions ($^{87}Sr/^{86}Sr$) are reported from 97 catchment outlet sediment samples from southwestern Australia (Yilgarn geological region). The analysed material originates from the sample archives of the National Geochemical Survey of Australia (NGSA) project, which targeted overbank or floodplain landforms near the
380 outlet of large catchments. The sampled catchments together cover 533 000 km^2 of southwestern Australia. For the most part (n = 107), bottom outlet sediment (BOS) samples, retrieved mostly by augering to, on average, 0.6 to 0.8 m depth, were analysed. Thirteen top outlet sediment (TOS) samples, collected from the top 0.1 m of soil, however, were also included. The BOS analyses are the focus of discussion in this paper. *Total* digestion of milled < 2 mm grain-size fractions from these sediments yielded a wide range of $^{87}Sr/^{86}Sr$ values from a minimum of 0.7152 to a maximum of 1.0909.
385 The present study presents one of the largest Sr isoscapes in the southern hemisphere, a region that is critically under-represented in terms of isotopic data worldwide. A map of the $^{87}Sr/^{86}Sr$ distribution (isoscape) across southwestern Australia reveals spatial patterns reflecting the ages and lithologies of the source material for the sediment, which is principally carried

down catchment by fluvial processes. The most radiogenic sediment values in the Yilgarn region (^{87}Sr/^{86}Sr > 0.8) all come from sites underlain by Archaean bedrock (2500 – 4000 Ma) and almost exclusively felsic intrusive lithologies. Conversely,

390 almost all sites underlain by younger *and* non-granitic bedrock have outlet sediments of a much less radiogenic character (^{87}Sr/^{86}Sr < 0.8). Sampling sites underlain by mafic and ultramafic bedrock sit at the intersection of these two trends, yielding unradiogenic Sr sediment signatures despite their Archaean age. Several sediment ^{87}Sr/^{86}Sr results were validated by comparing them to previously published whole-rock data from sites inside their catchment, for both unradiogenic and radiogenic cases.

395 The new Sr isotopic data are also interrogated in terms of the mineral occurrences (i.e., mineral deposits and/or operating mines) found in their catchment. Whilst over half of the ca 1000 mineral occurrences in the region originate from catchments with an intermediate ^{87}Sr/^{86}Sr signature (0.728 – 0.767), over 40 occurrences are associated with higher values (^{87}Sr/^{86}Sr > 0.8) and identified as outliers for various commodity groups (33 'Precious metals – Au, Ag'; four 'Iron ore'; two 'Battery/alloy metals – Ni, Co, Mn, V, Mo, Mg'; and one for each of 'Base metals – Cu (Zn, Pb, Ag, Au)'; 'Base metals – Zn, Pb (Cu, Ag)';

400 'Heavy mineral sands'; 'Other metals – Sn, Sb, W, Ta, Nb'; 'Rare earth elements'; and 'Uranium').

The southwestern Sr isoscape results are compared with two previously published, large-scale Sr isoscapes in Australia (southeastern and northern Australia), based on the same sample material and methods, and were found to have the highest median (0.7560) and maximum (1.0909) ^{87}Sr/^{86}Sr values of the three areas. Commonality of sampling and analytical protocols further allows the three Sr isotopic datasets to be combined into a preliminary national Sr isoscape, across vastly different

405 geological, ecological and topographic conditions, revealing regional Sr isotope patterns and trends, as well as anomalies, which could form the basis for a more complete national Sr isoscape and more detailed Sr isotope systematics studies in the future. Such work could extend the current focus on lithology, age and mineralisation influences, to studies of hydrology, food tracing, dust provenancing/sourcing, and historic migrations of people and animals.

410 **Supplement.** The supplement related to this article is available online at: https://doi.org/10.5194/essd-xx-xxxx-xxxx-supplement.

Author contributions. PdC provided the concept, samples, funding, data curation, analysis and visualisation, and manuscript writing and editing. AD provided technical guidance, resources and supervision, data curation, and manuscript editing. FD

415 provided technical support and data curation.

Competing interests. The contact author has declared that none of the authors has any competing interests.

Disclaimer. PdC publishes with the permission from the Chief Executive Officer, Geoscience Australia.

420

Acknowledgments See below.

425

Financial support. This research has been supported by the Australian Government's Exploring for the Future program (https://www.eftf.ga.gov.au/about, last access: 12 August 2024).

Acknowledgements

The National Geochemical Survey of Australia (NGSA) project would not have been possible without Commonwealth funding
430   through the Onshore Energy Security Program (http://www.ga.gov.au/ngsa, last access: 12 August 2024), and Geoscience Australia appropriation. Collaboration with the geoscience agencies of all states and the Northern Territory is gratefully recognised. We acknowledge all land owners and custodians, whether private, corporate, and/or traditional, for granting access to the field sites for the purposes of sampling. We thank Geoscience Australia laboratory staff for assistance with preparing the samples. Ivan Schroder (Geoscience Australia), Ian Moffat (Flinders University) and Jodie Pritchard (CSIRO) are thanked
435   for providing thoughtful reviews that have improved the original manuscript. Journal Editor Attila Demény is thanked for his professional handling of this submission.

Financial support

This research has been supported by the Australian Government (Exploring for the Future). Geoscience Australia's Exploring for the Future program provides precompetitive information to inform decision-making by government, community and
440   industry on the sustainable development of Australia's mineral, energy and groundwater resources. By gathering, analysing and interpreting new and existing precompetitive geoscience data and knowledge, we are building a national picture of Australia's geology and resource potential. This leads to a strong economy, resilient society and sustainable environment for the benefit of all Australians. This includes supporting Australia's transition to net zero emissions, strong, sustainable resources and agriculture sectors, and economic opportunities and social benefits for Australia's regional and remote communities. The
445   Exploring for the Future program, which commenced in 2016, is an eight year, $225m investment by the Australian Government.

References

Adams, S., Grün, R., McGahan, D., Zhao, J.-X., Feng, Y., Nguyen, A., Willmes, M., Quaresimin, M., Lobsey, B., Collard, M., and Westaway, M. C.: A strontium isoscape of north-east Australia for human provenance and repatriation, Geoarchaeol., 34, 450   231– 251, https://doi.org/10.1002/gea.21728, 2019.

Australian Soil Resource Information System (ASRIS): ASRIS Map Viewer Tool, Landcover Layer, Land Use Catchment Scale, https://www.arcgis.com/apps/mapviewer/index.html?url=https://asris.csiro.au/arcgis/rest/services/ASRIS/Landcover/MapServer&source=sd (last access: 12 August 2024), 2024.

455   Research Data Australia (RDA): Atlas of Australian Soils (digital) [data set], https://researchdata.edu.au/atlas-australian-soils-digital/1440573 (last access: 12 August 2024), 2024.

Bataille, C. P., Brennan, S. R., Hartmann, J., Moosdorf, N., Wooller, M. J., and Bowen, G. J.: A geostatistical framework for predicting variability in strontium concentrations and isotope ratios in Alaskan rivers, Chem. Geol., 389, 1–15, https://doi.org/10.1016/j.chemgeo.2014.08.030, 2014.

460   Bataille, C. P., Crowley, B. E., Wooller, M. J., and Bowen, G. J.: Advances in global bioavailable strontium isoscapes, Palaeogeogr. Palaeocl. Palaeoecol., 555, 109849, https://doi.org/10.1016/j.palaeo.2020.109849, 2020.

Bataille, C. P., von Holstein, I. C. C., Laffoon, J. E., Willmes, M., Liu, X.- M., and Davies, G. R.: A bioavailable strontium isoscape for Western Europe: a machine learning approach, PLoS ONE, 13(5), e0197386, https://doi.org/10.1371/journal.pone.0197386, 2018.

465   Blake, D. H. and Kilgour, B.: Geological Regions of Australia 1 : 5000 000 scale, Geosci. Austral., Canberra [data set], http://pid.geoscience.gov.au/dataset/ga/32366 (last access: 12 August 2024), 1998.

Bølviken, B., Bogen, J., Jartun, M., Langedal, M., Ottesen, R. T., and Volden, T.: Overbank sediments: a natural bed blending sampling medium for large-scale geochemical mapping, Chemometr. Intell. Lab., 74, 183–199, https://doi.org/10.1016/j.chemolab.2004.06.006, 2004.

470   Bureau of Meteorology (BOM): Climate classification maps, Köppen major classes, http://www.bom.gov.au/climate/maps/averages/climate-classification/?maptype=kpngrp (last access: 12 August 2024), 2024b.

Bureau of Meteorology (BOM): Climate classification maps, Temperature/humidity zones http://www.bom.gov.au/climate/maps/averages/climate-classification/?maptype=tmp_zones (last access: 12 August 2024), 475   2024a.

Bureau of Meteorology (BOM): Decadal and multi-decadal temperature, http://www.bom.gov.au/jsp/ncc/climate_averages/decadal-temperature/index.jsp?maptype=1&period=9605&product=min#maps (last access: 12 August 2024), 2024c.

Bureau of Meteorology (BOM): Recent and historical rainfall maps,
480 http://www.bom.gov.au/climate/maps/rainfall/?variable=rainfall&map=totals&period=48month®ion=nat&year=2009&month=11&day=30 (last access: 12 August 2024), 2024d.

Cooper, M., de Caritat, P., Burton, G., Fidler, R., Green, G., House, E., Strickland, C., Tang, J., and Wygralak, A.: National Geochemical Survey of Australia: Field Data, Record, 2010/18, Geosci. Austral., Canberra, https://doi.org/10.11636/Record.2011.020, 2010.

485 Crameri, F., Shephard, G. E., and Heron, P. J.: The misuse of colour in science communication, Nat Commun, 11, 5444, https://doi.org/10.1038/s41467-020-19160-7, 2020.

Crameri, F.: Scientific colour maps, Zenodo, https://doi.org/10.5281/zenodo.1243862, 2018.

Cutten, H. N., and Riganti, A., (compilers): 1:500 000 State Interpreted Bedrock Geology of Western Australia, Geological Survey of Western Australia, https://dasc.dmirs.wa.gov.au/, 2020.

490 de Caritat, P. and Cooper, M.: A continental-scale geochemical atlas for resource exploration and environmental management: the National Geochemical Survey of Australia, Geochem. Explo. Env. Anal., 16, 3–13, https://doi.org/10.1144/geochem2014-322, 2016.

de Caritat, P. and Cooper, M.: National Geochemical Survey of Australia: Data Quality Assessment, Record, 2011/21, Geosci. Austral., Canberra, http://pid.geoscience.gov.au/dataset/ga/71971 (last access: 12 August 2024), 2011b.

495 de Caritat, P. and Cooper, M.: National Geochemical Survey of Australia: The Geochemical Atlas of Australia, Record, 2011/20, Geosci. Austral., Canberra, http://dx.doi.org/10.11636/Record.2011.020 (last access: 12 August 2024), 2011a.

de Caritat, P., Cooper, M., Lech, M., McPherson, A., and Thun, C.: National Geochemical Survey of Australia: Sample Preparation Manual, Record, 2009/08, Geosci. Austral., Canberra, http://pid.geoscience.gov.au/dataset/ga/68657 (last access: 12 August 2024), 2009.

500 de Caritat, P., Cooper, M., Pappas, W., Thun, C., and Webber, E.: National Geochemical Survey of Australia: Analytical Methods Manual, Record, 2010/15, Geosci. Austral., Canberra, http://pid.geoscience.gov.au/dataset/ga/70369 (last access: 12 August 2024), 2010.

de Caritat, P., Dosseto, A., and Dux, F.: A strontium isoscape of inland southeastern Australia. Earth Syst. Sci. Data, 14, 4271–4286. https://doi.org/10.5194/essd-14-4271-2022, 2022.

505 de Caritat, P., Dosseto, A., and Dux, F.: A strontium isoscape of northern Australia. Earth Syst. Sci. Data, 15, 1655–1673. https://doi.org/10.5194/essd-15-1655-2023, 2023

de Caritat, P., Dosseto, A., and Dux, F.: A strontium isoscape of southwestern Australia, Geosci. Austral., Canberra [data set], https://dx.doi.org/10.26186/149755, 2024.

de Caritat, P.: The National Geochemical Survey of Australia: review and impact. Geochemistry: Exploration, Environment,
510 Analysis, geochem2022-032, https://doi.org/10.1144/geochem2022-032, 2022.

De Laeter, J. R., and Libby, W. G.: Early Palaeozoic biotite Rb-Sr dates in the Yilgarn Craton near Harvey, Western Australia, Aus. J. Earth Sci., 40, 445–453, https://doi.org/10.1080/08120099308728095, 1993.

Di Paola-Naranjo, R. D., Baroni, M. V., Podio, N. S., Rubinstein, H. R., Fabani, M. P., Badini, R. G., Inga, M., Ostera, H. A., Cagnoni, M., Gallegos, E., Gautier, E., Peral-Garcia, P., Hoogewerff, J., and Wunderlin, D. A.: Fingerprints for main varieties of Argentinean wines: terroir differentiation by inorganic, organic, and stable isotopic analyses coupled to chemometrics, J. Ag. Food Chem., 59, 7854–7865, https://doi.org/10.1021/jf2007419, 2011.

Frei, R. and Frei, K. M.: The geographic distribution of Sr isotopes from surface waters and soil extracts over the island of Bornholm (Denmark) – A base for provenance studies in archeology and agriculture, Appl. Geochem., 38, 147–160, https://doi.org/10.1016/j.apgeochem.2013.09.007, 2013.

Geoscience Australia (GA): Australia's River Basins 1997 – Product User Guide, Geosci. Austral., Canberra, http://pid.geoscience.gov.au/dataset/ga/42343 (last access: 12 August 2024), 1997.

Gosz, J. R., Brookins, D.G., and Moore, D.I.: Using strontium isotope ratios to estimate inputs to ecosystems, Biosci., 33, 23–30, https://doi.org/10.2307/1309240, 1983.

Hoogewerff, J. A., Reimann, C., Ueckermann, H., Frei, R., Frei, K. M., van Aswegen, T., Stirling, C., Reid, M., Clayton, A., Ladenberger, A., and The GEMAS Project Team: Bioavailable $^{87}Sr/^{86}Sr$ in European soils: a baseline for provenancing studies, Sci. Total Environ., 672, 1033–1044, https://doi.org/10.1016/j.scitotenv.2019.03.387, 2019.

Hutchinson, M. F., Stein, J. L., Stein, J. A., Anderson, H., and Tickle, P. K.: GEODATA 9 second DEM and D8: Digital Elevation Model Version 3 and Flow Direction Grid 2008. Record DEM-9S. v3. Geosci. Austral., Canberra [data set]. https://pid.geoscience.gov.au/dataset/ga/66006 (last access: 12 August 2024), 2008.

Isbell, R. F. and National Committee on Soil and Terrain: The Australian Soil Classification, third edn., CSIRO Publishing, Melbourne, Victoria, 181 pp., https://ebooks.publish.csiro.au/content/australian-soil-classification-9781486314782 (last access: 12 August 2024), 2021.

Joannes-Boyau, R., Adams, J. W., Austin, C., Arora, M., Moffat, I., Herries, A. I. R., Tonge, M. P., Benazzi, S., Evans, A. R., Kullmer, O., Wroe, S., Dosseto, A., and Fiorenza, L.: Elemental signatures of Australopithecus africanus teeth reveal seasonal dietary stress, Nature, 572, 112–115, https://doi.org/10.1038/s41586-019-1370-5, 2019.

Jweda, J., Bolge, L., Class, C., and Goldstein, S. L.: High precision Sr-Nd-Hf-Pb isotopic compositions of USGS reference material BCR-2, Geostand. Geoanal. Res., 40, 101–115, https://doi.org/10.1111/j.1751-908X.2015.00342.x, 2016.

Koutamanis, D., McCurry, M., Tacail, T., and Dosseto, A.: Reconstructing Pleistocene Australian herbivore megafauna diet using calcium and strontium isotopes, Royal Society Open Science, 10, 230991, https://doi.org/10.1098/rsos.230991, 2023.

Lech, M. E., de Caritat, P., and Mcpherson, A. A.: National Geochemical Survey of Australia: Field Manual, Record, 2007/08, Geosci. Austral., Canberra, http://pid.geoscience.gov.au/dataset/ga/65234 (last access: 12 August 2024), 2007.

McCulloch, M. T., Compston, W., and Froude, D.: Sm-Nd and Rb-Sr dating of Archaean gneisses, eastern Yilgarn Block, Western Australia, J. Geol. Soc. Aus., 30, 149–153, https://doi.org/10.1080/00167618308729242, 1983.

McNutt R. H.: Strontium Isotopes. In: Environmental Tracers in Subsurface Hydrology, edited by: Cook P. G. and Herczeg A. L., Springer, Boston, MA, https://doi.org/10.1007/978-1-4615-4557-6_8, 2000.

Moffat, I., Rudd, R., Willmes, M., Mortimer, G., Kinsley, L., McMorrow, L., Armstrong, R., Aubert, M., and Grün, R.: Bioavailable soil and rock strontium isotope data from Israel. Earth Syst. Sci. Data, 12, 3641–3652, https://doi.org/10.5194/essd-12-3641-2020, 2020.

Nebel O., Stammeier J. A.: Strontium Isotopes. In: Encycl. Geochem., Encycl. Earth Sci. Series, edited by: White W. M., Springer, Cham. https://doi.org/10.1007/978-3-319-39312-4_137, 2018.

Ottesen, R. T., Bogen, J., Bølviken, B., and Volden, T.: Overbank sediment: a representative sample medium for regional geochemical sampling, J. Geoch. Explo., 32, 257–277, https://doi.org/10.1016/0375-6742(89)90061-7, 1989.

Pacheco-Forés, S. I., Gordon, G. W., and Knudson, K. J.: Expanding radiogenic strontium isotope baseline data for central Mexican paleomobility studies, PLoS ONE, 15, e0229687, https://doi.org/10.1371/journal.pone.0229687, 2020.

Pain, C., Gregory, L., Wilson, P., and McKenzie, N.: The Physiographic Regions of Australia – Explanatory Notes, Australian Collaborative Land Evaluation Program (ACLEP) and National Committee on Soil and Terrain (NCST), Canberra, 30 pp., http://hdl.handle.net/102.100.100/104103?index=1 (last access: 12 August 2024), 2011.

Plumlee, G.: Basalt, Columbia River, BCR-2, Prelim. U.S. Geol. Surv. Cert. Anal., https://cpb-us-w2.wpmucdn.com/muse.union.edu/dist/c/690/files/2021/07/usgs-bcr2-1.pdf (last access: 12 August 2024), 1998.

Price, G. J., Ferguson, K. J., Webb, G. E., Feng, Y. X., Higgins, P., Nguyen, A. D., Zhao, J. X., Joannes-Boyau, R., and Louys, J.: Seasonal migration of marsupial megafauna in Pleistocene Sahul (Australia-New Guinea), P. Roy. Soc. B-Biol. Sci., 284, 20170785, https://doi.org/10.1098/rspb.2017.0785, 2017.

Romaniello, S. J., Field, M. P., Smith, H. B., Gordon, G. W., Kim, M. H., and Anbar, A. D.: Fully automated chromatographic purification of Sr and Ca for isotopic analysis, J. Anal. Atomic Spectro., 30, 1906–1912, https://doi.org/10.1039/C5JA00205B, 2015.

Rotenberg, E., Davis, D. W., Amelin, Y., Ghosh, S., and Bergquist, B. A.: Determination of the decay-constant of ^{87}Rb by laboratory accumulation of ^{87}Sr, Geochim. Cosmochim. Ac., 85, 41–57, https://doi.org/10.1016/j.gca.2012.01.016, 2012.

Senior, A., Britt, A., Summerfield, D., Hughes, A., Hitchman, A., Cross, A., Champion, D., Huston, D., Bastrakov, E., Sexton, M., Moloney, J., Pheeney, J., Teh M., and Schofield, A.: Australia's Identified Mineral Resources 2020. Geoscience Australia, Canberra, http://dx.doi.org/10.11636/1327-1466.2020, 2021.

Tukey, J. W.: Exploratory Data Analysis, Addison-Wesley Publishing Company, Reading, MA, 506 pp., 1977.

Vinciguerra, V., Stevenson, R., Pedneault, K., Poirer, A., Hélie, J.- F., and Widory, D.: Strontium isotope characterization of Wines from the Quebec (Canada) Terroir, Proc. Earth Planet. Sci., 13, 252–255, https://doi.org/10.1016/j.proeps.2015.07.059, 2015.

Voerkelius, S., Lorenz, G. D., Rummel, S., Quétel, C. R., Heiss, G., Baxter, M., Brach-Papa, C., Deters-Itzelsberger, P., Hoelzl, S., Hoogewerff, J., Ponzevera, E., Bocxstaele, M., and Van Ueckermann, H.: Strontium isotopic signatures of natural mineral waters, the reference to a simple geological map and its potential for authentication of food, Food Chem., 118, 933–940, https://doi.org/10.1016/j.foodchem.2009.04.125, 2010.

Washburn, E., Nesbitt, J., Ibarra, B., Fehren-Schmitz, L., and Oelze, V. M.: A strontium isoscape for the Conchucos region of highland Peru and its application to Andean archaeology, PLOS ONE 16, e0248209, https://doi.org/10.1371/journal.pone.0248209, 2021.

Wilford, J.: A weathering intensity index for the Australian continent using airborne gamma-ray spectrometry and digital terrain analysis, Geoderma, 183–184, 124–142, https://doi.org/10.1016/j.geoderma.2010.12.022, 2012.

Willmes, M., Bataille, C. P., James, H. F., Moffat, I., McMorrow, L., Kinsley, L., Armstrong, R.A., Eggins, S., and Grün, R.: Mapping of bioavailable strontium isotope ratios in France for archaeological provenance studies, Appl. Geochem., 90, 75–86, https://doi.org/10.1016/j.apgeochem.2017.12.025, 2018.

Willmes, M., McMorrow, L., Kinsley, L., Armstrong, R., Aubert, M., Eggins, S., Falguères, C., Maureille, B., Moffat, I., and Grün, R.: The IRHUM (Isotopic Reconstruction of Human Migration) database – bioavailable strontium isotope ratios for geochemical fingerprinting in France, Earth Syst. Sci. Data, 6, 117–122, https://doi.org/10.5194/essd-6-117-2014, 2014.